

Defect Engineering into Metal–Organic Frameworks for the Rapid and Sequential Installation of Functionalities

Hyojin Park,^{†,||} Seongwoo Kim,^{†,||} Byunghyuck Jung,[‡] Myung Hwan Park,[§] Youngjo Kim,[†] and Min Kim^{*,†,||}

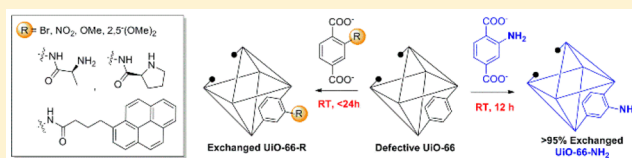
[†]Department of Chemistry and BK21Plus Research Team, Chungbuk National University, Cheongju, 28644, Republic of Korea

[‡]School of Basic Science, Daegu Gyeongbuk Institute of Science and Technology (DGIST), Daegu, 42988, Republic of Korea

[§]Department of Chemistry Education, Chungbuk National University, Cheongju, 28644, Republic of Korea

Supporting Information

ABSTRACT: Postsynthetic treatments are well-known and important functionalization tools of metal–organic frameworks (MOFs). Herein, we have developed a practical and rapid postsynthetic ligand exchange (PSE) strategy using a defect-controlled MOF. An increase in the number of defects amounts to MOFs with enhanced rates of ligand exchange in a shorter time frame. An almost quantitative exchange was achieved by using the most defective MOFs. This PSE strategy is a straightforward method to introduce a functionality into MOFs including bulky or catalytically relevant moieties. Furthermore, some mechanistic insights into PSE were revealed, allowing for a sequential ligand exchange and the development of multifunctional MOFs with controlled ligand ratios.



1. INTRODUCTION

Metal–Organic Frameworks (MOFs, also called porous coordination polymers, PCPs) are three-dimensional highly porous crystalline materials which consist of metal ions (or clusters) and multitopic organic ligands.^{1,2} Although the repeating coordination bonds between the secondary building units (SBUs) and the organic ligands produce infinite and identical pores, and MOFs are the thermodynamic product, structural defects are often found in the frameworks. In fact, defects, structural disorder, and heterogeneity of crystalline or solid-state materials are typical phenomena and have been widely studied for their physical and chemical properties in porous materials chemistry.^{3–5}

Among the various MOFs, MOF-5, HKUST-1, and UiO-66 (HKUST = Hong Kong University of Science and Technology, UiO = University of Oslo) are the most actively studied targets for defects in the framework.³ The zinc-based MOF-5 and the copper-based HKUST-1 are legacy MOFs and have been known since the late 1990s.^{6,7} The zirconium-based UiO-66 was first reported by Lillerud and co-workers in 2008 and has superior chemical and physical capabilities to both MOF-5 and HKUST-1.⁸ Additionally, the wide range of available functionalizations makes UiO-66 one of the most popular MOFs.⁹ Since UiO-66 is relatively robust and thought of as an “inert” material, it is hypothesized to be one of the most tolerant MOFs for both defect generation and engineering. Recently, Behrens and co-workers reported a practical synthesis of a UiO series with an acid modulator (i.e., monocarboxylic acid such as acetic acid or benzoic acid),¹⁰ and related studies have revealed that the acid modulators promote defect generation in the frameworks without the loss of the bulk crystallinity.^{11–15}

There are two main types of defects that have been hypothesized in the UiO-66 frameworks: “a vacancy of an organic linker” and “a vacancy of an entire SBU”.^{16,17} Both defects in UiO-66 were discovered and intensively studied by multiple research groups for their applications in molecular adsorption and catalysis.^{18–22} Very recently, Lillerud and co-workers reported the quantity of defects could be controlled by judicious choice of modulators.¹³ Both the amount of and the acidity (i.e., pK_a of acid) of an acid modulator are directly correlated to the number of defects formed as evidenced by N_2 adsorption, 1H NMR, PXRD (powder X-ray diffraction), and TGA (thermogravimetric analysis). During the defect controls, the most defective UiO-66 (from 36 equiv of trifluoroacetic acid as the modulator) showed a 50% higher BET (Brunauer–Emmett–Teller) surface area than the standard UiO-66 from traditional synthesis conditions (~ 1800 m^2/g than ~ 1200 m^2/g , respectively).

It is relatively easy to introduce not only defects but also a variety of functional groups affecting the strength and robustness of the UiO-66 frameworks. Various functional groups such as NH_2 , NO_2 , naphthyl, and Br have been directly incorporated into UiO-66 using a prefunctionalized ligand (i.e., direct synthesis), and amide/cyanide functionalities have been installed through postsynthetic modification (PSM) strategies.⁹ Lastly, postsynthetic ligand exchange (PSE) has also been applied to UiO-66 frameworks, and several interesting functionalities (e.g., azide - thermally unstable in solvothermal conditions, dihydroxy - strongly coordinates to the zirconium

Received: September 18, 2017

precursor) have been successfully introduced into UiO-66 frameworks.^{23,24} However, in this last case, the exchange rate was quite slow, rendering this particular PSE unpractical due to the lack of efficiency. Typically, only an ~50% exchange ratio was obtained for a functionalized BDC (benzene-1,4-dicarboxylic acid) ligand after 5 days.

Another strategy to introduce new functional groups through defects in MOFs has been recently attempted. Farha and Hupp's research team has successfully installed free-carboxylic acid groups in the copper-based NU-125 MOF (NU = Northwestern University). The solvent-assisted linker exchange (SALE) strategy was applied to defects in NU-125 for introducing BTC (benzene-1,3,5-tricarboxylic acid) ligands.²⁵ Additionally, a monoethanolamine moiety was incorporated into a UiO-66 framework for CO₂ capture using PSE by Zhang et al.²⁶ The defect sites in UiO-66 were generated by monodentate acid modulators, and then new functionalities, such as serine, were installed into those defect sites.²⁷ Inspired by three independent works, we investigated the correlation between the amount of defects and postsynthetic ligand exchange rates to install external functionalities into MOF pores. Moreover, we hypothesized that the presence of defects in MOFs could actually enhance the "ligand exchange strategy" and make it a more practical method for functionalization.

2. RESULTS AND DISCUSSION

Defect Controls for Postsynthetic Ligand Exchange Rates. We chose three different defect-controlled UiO-66 samples from Lillerud's system. No acid modulator was used for the standard UiO-66 synthesis (UiO-66(NA), BET surface area = ~1200 m²/g), 6 equiv of formic acid was used for UiO-66(FA) synthesis (BET surface area = ~1400 m²/g), and last, 36 equiv of trifluoroacetic acid was used for UiO-66(TFA) synthesis (BET surface area = ~1800 m²/g). These three samples were prepared by following reported procedures including activating and washing steps.¹³ As a model reaction, BDC-NH₂ and BDC-Br were used for PSE using these defect-controlled UiO-66 samples. The exchange was performed in aqueous conditions at room temperature, and the concentration of the ligand was fixed at 0.1 M for direct comparison with previous studies.²³ Surprisingly, the ligand exchange rates dramatically increased from the standard UiO-66(NA) and previous nondefective UiO-66 (i.e., synthesized UiO-66 sample without using an acid modulator and water).

The amount exchanged (at 3, 6, 12, and 24 h) was determined by ¹H NMR analysis after acid digestion using fully washed and activated samples (with water and methanol for 3 days; see the [Supporting Information](#) for details). While 51 ± 2% of BDC-NH₂ was incorporated into UiO-66(NA), a total of 74 ± 1% of BDC-NH₂ and 76 ± 1% of BDC-NH₂ were exchanged into UiO-66(FA) and UiO-66(TFA) in 24 h, respectively (average numbers from two independent samples, [Figures 1](#) and [S1–S6](#)). Once again, in the previous studies, pristine UiO-66 showed ~60% exchange after 5 days.²³ Additionally, we have investigated anion effects on PSE. Since the hydrolyzed dicarboxylate was neutralized with aqueous HCl solution, the exchanging solution has chloride ions. By modifying the acidification agent from HCl (aq.) to H₂SO₄ (aq.), the existing anion is changed to a sulfate ion. In this sulfate condition, 74% of BDC-NH₂ was incorporated into UiO-66(TFA) in 24 h, which is about the same amount as with the chloride ions ([Figure S7](#)).

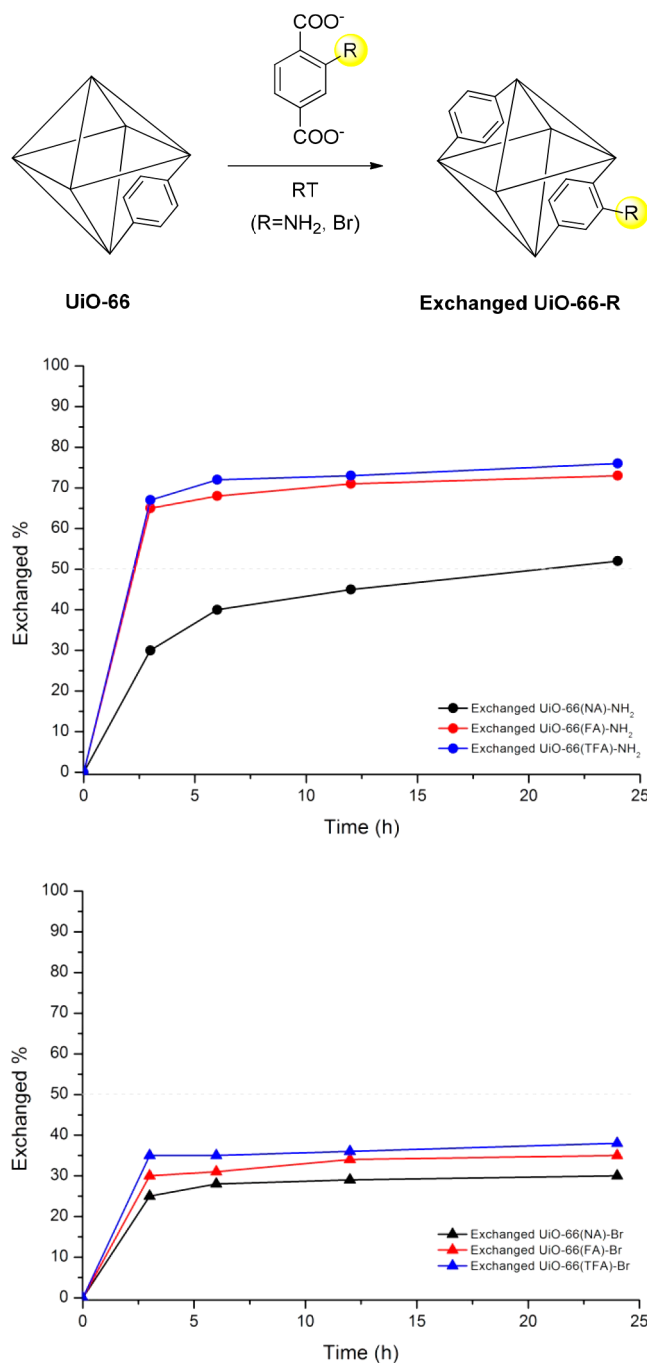


Figure 1. Ligand exchange rate and saturation level of BDC-NH₂ and BDC-Br into defect-controlled UiO-66s.

We believe that there is a chance for both ligand insertion into defect sites and true ligand exchange. However, the amount of exchange (76%) is much larger than the amount of available defects. In the previous study, it was reported that only 11% of the ligand was changed to the defect site in UiO-66(NA), 15% for UiO-66(FA), and 33% for UiO-66(TFA), respectively.¹³ To confirm the relative contribution of ligand insertion into the defect site, and overall ligand exchange, first, we compared the existing amount of both ligands (non-functionalized BDC and functionalized BDC) in the solid state (i.e., exchanged UiO-66) and in the aqueous media at the early stage of exchange before saturation. At 3 h, BDC-NH₂ was 60% incorporated into UiO-66(TFA) frameworks, and the

Table 1. Initial Ligand Exchange Rate (at 3 h) for BDC-NH₂ and BDC-Br for Defect-Controlled UiO-66s

exchanged ligand	UiO-66 ^a (%/h)	UiO-66(NA) (%/h)	UiO-66(FA) (%/h)	UiO-66(TFA) (%/h)
BDC-NH ₂	3.3	10	22	22
BDC-Br	2.5	8.3	10	12

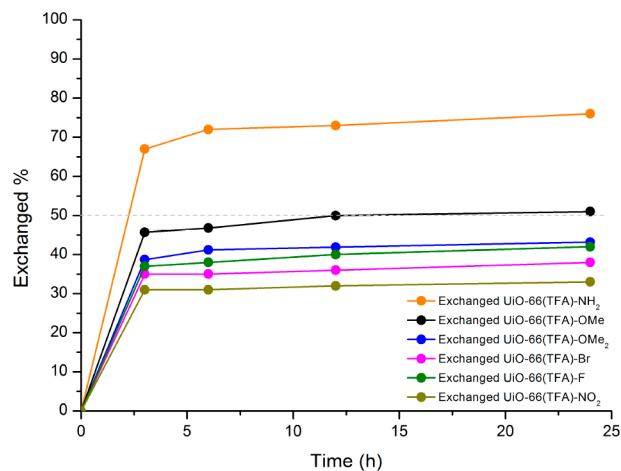
^aSynthesized without acid modulator and water. Data were obtained from ref 23.

BDC:BDC-NH₂ ratio was determined to be 40:60 in the solid state (Figure S8). Interestingly, a similar 40:60 ratio for BDC:BDC-NH₂ was observed in the remaining aqueous solution after exchange. This suggests that the amount of BDC exchanged out is ~20% less than the exchanged in BDC-NH₂. We believe that this difference stems from direct ligand insertion into the defect site without removing ligands. We have taken this a step further and utilized internal standards for our NMR studies to determine the definitive amount of defects, addition of ligands, and exchange. Before PSE, the chemical formula of UiO-66(TFA) is determined to be Zr₆O₄(OH)₄(BDC)_{4.17}. Since the chemical formula of defect-free UiO-66 is Zr₆O₄(OH)₄(BDC)₆, approximately 30% of the BDC ligand thought to be missing (i.e., the amount of defect) was confirmed, and this number is corroborated with a previously reported analysis by Lillerud using TGA.¹³ After PSE with NH₂-BDC for 6 h, a total of 76% of the ligand was exchanged and the formula of the exchanged sample was determined to be Zr₆O₄(OH)₄(BDC)_{1.59}(BDC-NH₂)_{3.10} (Figure S9). This means that, after PSE, the exchanged UiO-66(TFA)-NH₂ sample has approximately 20% defect sites. In other words, around 1/3 of the defect sites had an inserted ligand. Although both defect calculations, from NMR-internal standard and TGA, are not highly accurate,²⁸ this data strongly indicates that both ligand exchange and insertion processes exist in the defect-induced PSE process. This phenomenon was also observed in the case of UiO-66(FA) (Figures S9 and S10, and Table S1).

The incorporated ligand ratios were at least 2 times larger than the amount of defects at the early stage (<3 h), and we assumed that both UiO-66(FA) and UiO-66(TFA) displayed the maximum, saturated exchange amount for BDC-NH₂ (~70%/1 d). Figure 1 clearly displays that there are limits on the BDC-NH₂ exchange amount when using 1 equiv of additional ligand. Both UiO-66(FA) and UiO-66(TFA) reached the exchange saturation point within 5 h. In the case of BDC-Br, it generally showed lower exchange rates and amounts than BDC-NH₂, which is the same trend as was first reported.²³ As expected, UiO-66(NA) showed the lowest exchange amount at 30 ± 1% after 24 h, while UiO-66(FA) and UiO-66(TFA) showed 35 ± 1% and 39 ± 1%, respectively (average numbers from two independent samples, Figures S11–S16). Before the exchange saturation (at ~3 h), the exchange rates were compared and followed exactly the same trends with the maximum exchange amount (Table 1). In all cases, the UiO-66 framework is completely intact after ligand exchange as evidenced by PXRD patterns (Figure S17).

Functional Group Effects on Saturation Levels of Postsynthetic Ligand Exchange. To determine which factors influence the exchange rate and amount, the functional group effects were also investigated using a variety of ligands. Electron donating groups (EDG)-containing BDCs, BDC-OMe, and BDC-(OMe)₂ were prepared and utilized to probe both the electronic effects and the steric issues using UiO-66(TFA). Since a basic condition (aq. KOH) was employed for the hydrolysis step during PSE, the alkoxy group was

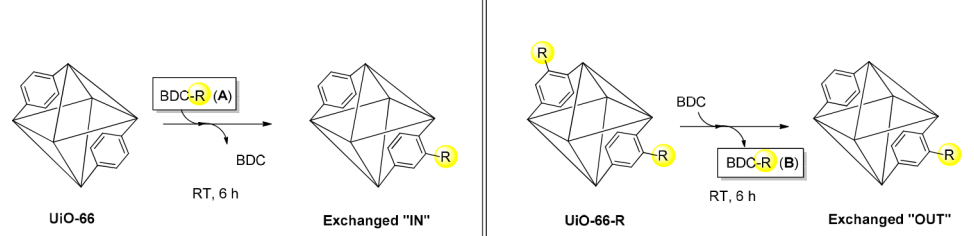
incorporated and the acidic phenol derivatives, such as BDC-OH and BDC-(OH)₂, were not selected in this study. EDGs (NH₂, OMe, and (OMe)₂) generally showed faster exchange rates and higher exchange amounts than electron-withdrawing groups (EWGs; F, Br, and NO₂), which are displayed in Figure 2. Among the EDGs, the amino group showed the highest

**Figure 2.** Ligand exchange rates and saturation level of functionalized ligands to UiO-66(TFA).

exchange amount (76 ± 1% exchanged, Figure S5), methoxy was in the middle (50 ± 1% exchanged, Figures S18 and S19), and the dimethoxy group demonstrated the lowest amount (43 ± 1% exchanged, Figures S20 and S21) for PSE into UiO-66(TFA). This indicates that the nucleophilicity of the carboxylate in the BDC ligand may play a key role in the PSE process (comparing rates between NH₂ > OMe), and the size of the functional group also contributed to the PSE rates (comparing methoxy > dimethoxy). In the opposite case, three EWGs (F, Br, and NO₂) showed slower PSE rates and lower exchange amount than the EDGs, and generally, these three examples show no significant differences during PSE (F-43 ± 1%, Br-39 ± 1%, and NO₂-33 ± 1% exchanged; average numbers from two independent samples, Figures 2, S11–S16, and S22–S25). In both EDG and EWG ligand exchange cases, the structure of UiO-66 was retained, which is evidenced by PXRD (Figures S17 and S26).

The first step of PSE is the attack of the dicarboxylate toward the zirconium clusters. In the case of UiO-66, a ligand dissociation first (i.e., without the nucleophilic attack of the dicarboxylate) will not likely occur since UiO-66 is a “relatively robust” and “chemically stable” MOF. Then, the observation here is very reasonable; the EDG makes the BDC a better nucleophile toward the metal cluster for initiating the exchange process. This suggests that an electronic factor of substituent is more prominent than the size factor, since size-different BDC-F and BDC-Br showed similar exchange rates and amounts in the defect-controlled PSE process (Figure 2).

Table 2. Exchanged Ratio for Both Functionalized Ligand Exchanged “IN” and “OUT” (at 6 h)



entry	R	ratio of exchanged “IN” (A) (%)	ratio of exchanged “OUT” (B) (%)
1	NH ₂	76 ± 1	33 ± 1
2	OMe	50 ± 1	49 ± 1
3	(OMe) ₂	43 ± 1	58 ± 1
4	Br	39 ± 1	60 ± 1
5	NO ₂	33 ± 1	64 ± 1

Effects of Functional Groups on the Parent MOFs.

From another perspective, to confirm the nucleophilicity of ligands, and the effects of coordination bond strength on the levels of PSE, we have examined the functional group effect on the parent MOFs with regards to PSE (Table 2). The functional group effect on the strut molecule was monitored when nonfunctionalized BDC was incorporated into the prefunctionalized UiO-66-R framework via PSE. The functionalized UiO-66-NH₂(as), UiO-66-OMe(as), UiO-66-(OMe)₂(as), UiO-66-Br(as), and UiO-66-NO₂(as) (as = as synthesized) were synthesized by solvothermal conditions with HCl as a modulator since TFA as a modulator is not ideal for functionalized UiO-66 synthesis. All functionalized UiO-66-R displayed identical frameworks evidenced by PXRD (Figure S27).

From the 6 h incubation at room temperature, the exchanged amounts generally showed a reverse trend to the previous exchange “IN” study (Table 2). The most nucleophilic BDC-NH₂ showed lower levels of exchange out of the framework by additional nonfunctionalized BDC (entry 1(B), Table 2, Figure S28). At the same time, the less nucleophilic BDC-Br and BDC-NO₂, which had shown the lowest exchanged amount in the previous functionalization study, showed the highest amount of exchange, 60% and 64%, respectively (entries 4(B) and 5(B) in Table 2, Figures S29 and S30). Both methoxy and dimethoxy substituted ligands showed similar ratio for both exchanged in and exchanged out experiments (Figures S31 and S32). Most interestingly, similar ligand ratios were obtained from either exchanged “IN” or exchanged “OUT” experiments. For example, installation of BDC-Br into a nonfunctionalized UiO-66 by an exchanged “IN” experiment provides BDC: 60% and BDC-Br: 40% incorporated into the UiO-66 framework. In the opposite case, installation of BDC into the prefunctionalized UiO-66-Br by being exchanged “OUT” gives a similar BDC: 60% and BDC-Br: 40% incorporation. This suggests that the exchange ratio is determined by the nature of ligands and an equilibration process with the MOF framework, and this finding clearly indicates that the coordination bond strength between the SBU and ligand plays a key role in the PSE process. These kinds of substituent effects on the metal-carboxylate complexes are rarely reported in the literature.²⁹ The electron-rich benzene ring (i.e., EDG-substituted ligand such as BDC-NH₂, BDC-OMe, and BDC-(OMe)₂) provides more electron density into the carboxylate, and these ligands are strongly coordinated to the zirconium ion on the SBU. Thus, the exchanged amount of

“exchanged IN” is much higher for BDC-NH₂ versus the “exchanged OUT” which is much lower in comparison to more electron deficient ligands, BDC-Br or BDC-NO₂. The structure of the UiO-66 framework was completely retained in both the exchanged “IN” and “OUT” for all cases, which was evidenced by PXRD (Figure S27).

Full Exchange and Various Functionalization through Postsynthetic Ligand Exchanges. Knowing that the existence of defects accelerates the PSE process, full ligand exchange was further examined by altering the number of exchanges and the exchange time (Figure 3). Both soaking with 3 equiv of BDC-NH₂ (for 24 h) or two times soaking 1 equiv of BDC-NH₂ (for 3 h + 9 h) for UiO-66(TFA) was attempted at room temperature, and both protocols produced ~95% exchanged UiO-66 frameworks from the nonfunctionalized

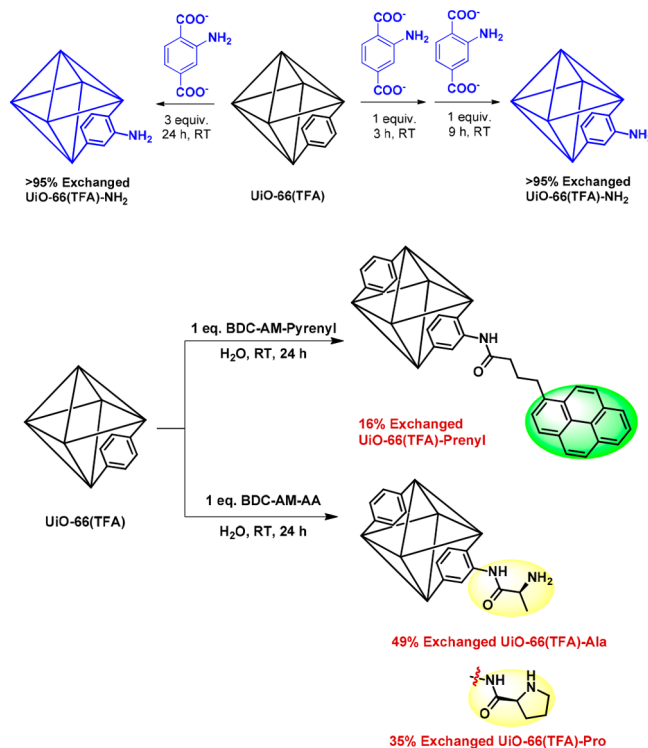


Figure 3. Full ligand exchange and biologically relevant ligand exchanges on defective UiO-66.

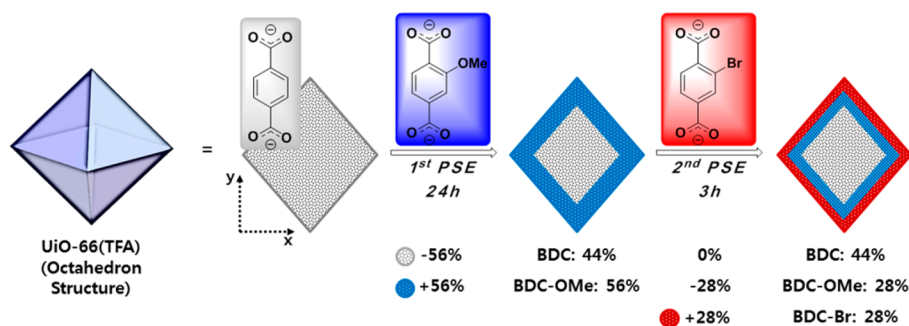


Figure 4. A sequential two-step PSE using BDC-OMe and BDC-Br from nonfunctionalized UiO-66(TFA).

UiO-66(TFA) (Figures S33 and S34). The ~95% exchanged UiO-66(TFA)-NH₂ generally displayed similar characteristics to the directly synthesized UiO-66(TFA)-NH₂ except for ¹H NMR after acid digestion. The PXRD and TGA data are identical for both exchanged and synthesized samples along with previously reported patterns (Figures S35 and S36).³⁰ The BET surface area for the exchanged UiO-66(TFA)-NH₂ was 1452 m²/g versus the synthesized UiO-66(TFA)-NH₂ which was 1217 m²/g, and the N₂ and CO₂ isotherms followed typical UiO-66-NH₂ patterns (Figures S37 and S38). However, several impurity peaks were observed during the ¹H NMR analysis after acid digestion. Since the exchanged UiO-66(TFA)-NH₂ showed only BDC, BDC-NH₂ peaks and remaining solvent peaks after the same activation treatment, the impurities in the synthesized samples must be caused from the solvothermal conditions (Figure S34). In the case of sensitive functional group-containing ligands, the strong acid modulator (e.g., TFA) condition is not a good method for preparing functionalized MOFs and may have degraded the ligands as we observed. Additionally, the increased surface area of UiO-66(TFA)-NH₂ corroborates the existence of remaining defects in the exchanged UiO-66 framework. The PSE process is not a dissolution/recrystallization mechanism which is evidenced by PXRD, TGA, ex situ ¹H NMR, solid-state NMR, and computational studies by several groups.^{24,31,32} This fully exchanged result lends weight to the importance of MOF dynamics and the speed of the ongoing exchange equilibrium.

With this fast and convenient ligand installation strategy in our hands, as a proof-of-concept study, we thought to install a bulky ligand that is typically unable to be incorporated into UiO-66 frameworks through a direct synthesis. This pyrene-based ligand was prepared through an amide coupling reaction as a model substrate and applied to the PSE. Interestingly, 16% ligand exchange was monitored with a retained UiO-66 framework, and the exchange ratio was not increased by either additional exposure or exchange time (16% for 72 h, Figures S39 and S40). This result suggests that only surface exchange occurred; the sterically bulky pyrenyl ligand could only fit on the surface of the UiO-66 crystal and did not penetrate to the inside of the pores for further PSE. As the exchanged pyrenyl ligands potentially blocked the diffusion channel for other ligands, or the side chain made the BDC ligand simply too large to fit through the pores, PSE was limited to only the exterior part of the UiO-66 crystal. Lastly, the more biologically relevant amino acid-containing BDCs installation was performed utilizing a defective UiO-66. BDC-AM-Ala and BDC-AM-Pro were prepared and applied to PSE functionalization. Both amino acid derivatives displayed moderate exchange amounts (49 ± 1% and 34 ± 1% for BDC-AM-Ala and BDC-AM-Pro

respectively, Figures S41 and S42), and once again, the structure of UiO-66 was completely retained after the BDC-AM-Pyrenyl and amino acid-BDC exchange process (Figure S43).

Sequential Ligand Exchange and Core/Shell Type MOFs. The early saturation of the BDC-AM-Pyrenyl exchange in conjunction with the lower exchange amount of BDC-AM-Pro over BDC-AM-Ala strongly suggests that the PSE process is still controlled by the size of the substituent when it is larger than the available diffusion channel in MOF. It also implies that the PSE process starts at the surface of MOF and does not proceed through the whole particle at the same time.³⁴ To verify this PSE mechanism, we have designed a sequential two-step PSE (Figure 4). Nonfunctionalized UiO-66(TFA) was first exchanged with BDC-OMe and a 56% exchanged sample was obtained. If the PSE process occurred from the surface inward, the core of the particle would have 44% nonfunctionalized BDC remaining. Starting from this exchanged MOF, a second PSE using BDC-Br was performed. As a result, 28% of BDC-Br was incorporated into UiO-66 by the second PSE. Surprisingly, only 28% of the previously installed BDC-OMe was exchanged out and none of the BDC had exchanged with BDC-Br (Figures 4, S44 and S45). We believe that this is a strong evidence for the directionality of PSE, beginning from the accessible surface and working toward the core of the MOF. And this is a very interesting three-layered core-shell structure of MOFs with three different ligands. Previously, the growth of the second MOF on the first seed MOF for constructing core-shell or hetero-compositional MOFs has been studied with several specific examples, and our finding supports that the sequential PSE of MOFs is a practical way for preparation of a core-shell structure on MOFs.^{33–40}

Additionally, other mechanistic details were revealed during time-controlled sequential PSE experiments. By increasing the 2nd PSE exposure time to 24 h, we observed a decrease of the core part and a leaching out of nonfunctionalized BDC totaling 9%. In other words, the exchanged “free” BDC-OMe by BDC-Br on the pore near the surface had penetrated into the core during the elongated reaction time and some exchange between BDC-OMe and the nonfunctionalized BDC had occurred (Figures 5, S46, and S47). The PXRD pattern was totally intact even after the 24 h/24 h sequential PSE (Figure S48). To summarize, these two results strongly support that the PSE process is not a dissolution/recrystallization mechanism and follows a diffusion/replacement mechanism throughout the MOF particle since the PSE ratio was affected by the PSE sequence.^{31,32}

This sequential PSE has been developed as a practical method for preparing multifunctional MOFs. From a previous

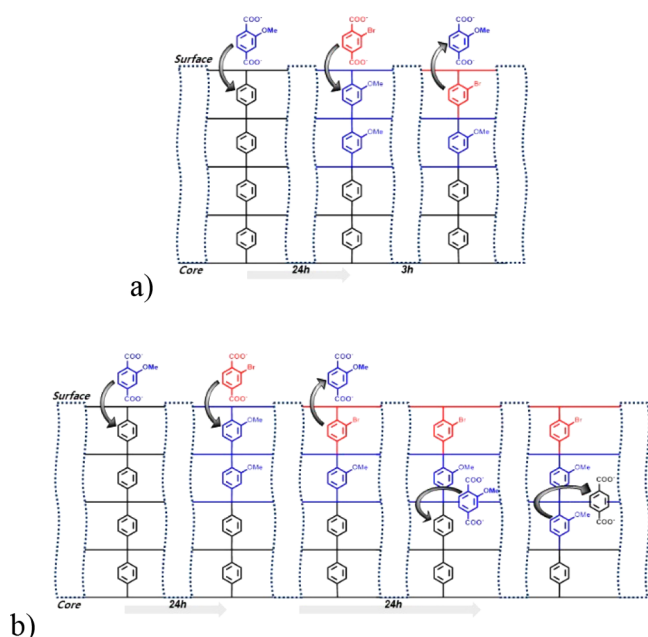


Figure 5. Time-controlled sequential PSE for diffusion mechanism confirmation: (a) short time (3 h) for 2nd PSE and (b) long time (24 h) for the 2nd PSE.

study, a mixed ligand strategy allows a maximum of eight different functionalities into a single MOF pore with a random distribution via direct synthesis.⁴¹ In contrast; this sequential PSE could be also used to prepare multiple functionalities within the MOF pores but potentially with a gradient of functional groups from the inside out.

3. EXPERIMENTAL SECTION

Preparation of Defect-Controlled UiO-66s. The UiO-66 series was prepared and activated using a modified method from what has been previously described.¹³

UiO-66(TFA). Terephthalic acid (123 mg, 0.74 mmol), $ZrCl_4$ (172 mg, 0.74 mmol), DMF (20 mL), H_2O (0.040 mL, 2.22 mmol), and trifluoroacetic acid (2.04 mL, 26.6 mmol) were placed in a Teflon lined autoclave and heated at 120 °C for 72 h. The microcrystalline powders were isolated by centrifugation. Residual DMF and ligand precursors were removed from the material by washing with 12 mL of DMF three times. Then they were incubated with fresh DMF (12 mL) for overnight at 70 °C. Three further such washes were performed. Then the solids were washed with 3×12 mL of MeOH, after which the solids were left to soak in 12 mL of MeOH for 1 day. The solids were centrifuged and dried under vacuum.

General Procedures of Postsynthetic Ligand Exchange (PSE). Functionalized ligand (0.1 mmol, 0.1 M) was dissolved in THF (1 mL) and aqueous 4% KOH solution (1 mL). The solution was stirred at room temperature overnight. The THF was removed by evaporation, and the remaining aqueous phase was neutralized to pH 7 with 1 M HCl solution. This solution was added to UiO-66 (ca. 29 mg, 0.1 mmol of BDC), and the mixture was incubated at room temperature. After finishing the exchange, the mixture was centrifuged and the aqueous phase decanted. The solids were suspended in 5 mL of water, and solid was centrifuged and the water was decanted. This water washing was repeated for two times. After water washing, the solids were washed with 5 mL of MeOH (two times). Then the solids were suspended in 5 mL of MeOH. After 24 h, the solid was centrifuged and MeOH was decanted. This MeOH soaking step was repeated two more times (for 24 h each). The solid phase was finally dried under vacuum for 6 h.

4. CONCLUSIONS

In conclusion, we have developed a practical and rapid postsynthetic ligand exchange strategy using a modulator-induced, defect-controlled UiO-66 system. Increase of the defect amounts in the MOF pore enhances the ligand exchange rate and ratio in a shorter time frame. In particular, using either 3 equiv of functionalized ligands, or 2 times a single equivalent, for the exposure, solution produces an almost fully exchanged ratio for the most defective UiO-66(TFA) in 12 h at room temperature (previous report was ~60% exchange for 5 days). This strategy is also a straightforward method to introduce bulky or catalytically useful functionalities into MOFs. The pyrenyl-containing BDC was successfully incorporated into the UiO-66 framework through PSE only on the surface, while the amino acid groups were successfully installed into the UiO-66 pores. By examining a variety of functionalities for PSE, we have identified two important mechanistic parameters: the electronic density of the benzene ring is highly correlated with the exchange rate, and the size of the pendant substituent is also essential. Leveraging the surface first exchange, a sequential PSE was developed to prepare multifunctional MOFs with a subtler gradient of functionalities in comparison to a core-shell MOF. This synthetic strategy offers an exciting opportunity to the preparation of diverse water and chemically stable MOFs with a wide range of functionalities which are desirable for various applications.

■ ASSOCIATED CONTENT

Supporting Information

The Supporting Information is available free of charge on the ACS Publications website at DOI: 10.1021/acs.inorgchem.7b02391.

Detailed procedures for ligand synthesis, figures, and a table as described in the text and 1H and ^{13}C NMR and IR spectra (PDF)

■ AUTHOR INFORMATION

Corresponding Author

*E-mail: minkim@chungbuk.ac.kr.

ORCID

Myung Hwan Park: 0000-0002-8858-5204

Youngjo Kim: 0000-0001-8571-0623

Min Kim: 0000-0002-1710-2682

Author Contributions

The manuscript was written through contributions of all authors. All authors have given approval to the final version of the manuscript. These authors contributed equally.

Notes

The authors declare no competing financial interest.

■ ACKNOWLEDGMENTS

We thank Dr. Corinne A. Allen (AAAS Science & Technology Policy Fellow at the Department of Energy, USA) for helpful discussions and in preparing this manuscript. This research was supported by the Science Research Center (2016R1A5A1009405) and Basic Science Research Program (2016R1C1B1011076) through the National Research Foundation of Korea (NRF) funded by the Ministry of Science, ICT & Future Planning.

REFERENCES

- (1) Zhou, H.-C.; Long, J. R.; Yaghi, O. M. Introduction to Metal-Organic Frameworks. *Chem. Rev.* **2012**, *112*, 673–674.
- (2) Ockwig, N. W.; Delgado-Friedrichs, O.; O’Keeffe, M.; Yaghi, O. M. Reticular Chemistry: Occurrence and Taxonomy of Nets and Grammar for the Design of Frameworks. *Acc. Chem. Res.* **2005**, *38*, 176–182.
- (3) Fang, Z.; Bueken, B.; De Vos, D. E.; Fischer, R. A. Defect-Engineered Metal–Organic Frameworks. *Angew. Chem., Int. Ed.* **2015**, *54*, 7234–7254.
- (4) Cheetham, A. K.; Bennett, T. D.; Coudert, F.-X.; Goodwin, A. L. Defects and disorder in metal organic frameworks. *Dalton Trans.* **2016**, *45*, 4113–4126.
- (5) Bennett, T. D.; Cheetham, A. K.; Fuchs, A. H.; Coudert, F.-X. Interplay between defects, disorder and flexibility in metal-organic frameworks. *Nat. Chem.* **2017**, *9*, 11–16.
- (6) Li, H.; Eddaoudi, M.; O’Keeffe, M.; Yaghi, O. M. Design and synthesis of an exceptionally stable and highly porous metal-organic framework. *Nature* **1999**, *402*, 276–279.
- (7) Chui, S. S.-Y.; Lo, S. M.-F.; Charmant, J. P. H.; Orpen, A. G.; Williams, I. D. A Chemically Functionalized Nanoporous Material [Cu₂(TMA)₂(H₂O)₃]_n. *Science* **1999**, *283*, 1148–1150.
- (8) Cavka, J. H.; Jakobsen, S.; Olsbye, U.; Guillou, N.; Lamberti, C.; Bordiga, S.; Lillerud, K. P. A New Zirconium Inorganic Building Brick Forming Metal Organic Frameworks with Exceptional Stability. *J. Am. Chem. Soc.* **2008**, *130*, 13850–13851.
- (9) Kim, M.; Cohen, S. M. Discovery, development, and functionalization of Zr(IV)-based metal–organic frameworks. *CryStEngComm* **2012**, *14*, 4096–4104.
- (10) Schaate, A.; Roy, P.; Godt, A.; Lippke, J.; Waltz, F.; Wiebcke, M.; Behrens, P. Modulated Synthesis of Zr-Based Metal–Organic Frameworks: From Nano to Single Crystals. *Chem. - Eur. J.* **2011**, *17*, 6643–6651.
- (11) Gutov, O. V.; Hevia, M. G.; Escudero-Adan, E. C.; Shafir, A. Metal–Organic Framework (MOF) Defects under Control: Insights into the Missing Linker Sites and Their Implication in the Reactivity of Zirconium-Based Frameworks. *Inorg. Chem.* **2015**, *54*, 8396–8400.
- (12) Hu, Z.; Castano, I.; Wang, S.; Wang, Y.; Peng, Y.; Qian, Y.; Chi, C.; Wang, X.; Zhao, D. Modulator Effects on the Water-Based Synthesis of Zr/Hf Metal–Organic Frameworks: Quantitative Relationship Studies between Modulator, Synthetic Condition, and Performance. *Cryst. Growth Des.* **2016**, *16*, 2295–2301.
- (13) Shearer, G. C.; Chavan, S.; Bordiga, S.; Svelle, S.; Olsbye, U.; Lillerud, K. P. Defect Engineering: Tuning the Porosity and Composition of the Metal–Organic Framework UiO-66 via Modulated Synthesis. *Chem. Mater.* **2016**, *28*, 3749–3761.
- (14) Atzori, C.; Shearer, G. C.; Maschio, L.; Civalieri, B.; Bonino, F.; Lamberti, C.; Svelle, S.; Lillerud, K. P.; Bordiga, S. Effect of Benzoic Acid as a Modulator in the Structure of UiO-66: An Experimental and Computational Study. *J. Phys. Chem. C* **2017**, *121*, 9312–9324.
- (15) Cai, G.; Jiang, H.-L. A Modulator-Induced Defect-Formation Strategy to Hierarchically Porous Metal–Organic Frameworks with High Stability. *Angew. Chem.* **2017**, *129*, 578–582.
- (16) Cliffe, M. J.; Wan, W.; Zou, X.; Chater, P. A.; Kleppe, A. K.; Tucker, M. G.; Wilhelm, H.; Funnell, N. P.; Coudert, F.-X.; Goodwin, A. L. Correlated defect nanoregions in a metal–organic framework. *Nat. Commun.* **2014**, *5*, 4176.
- (17) Trickett, C. A.; Gagnon, K. J.; Lee, S.; Gandara, F.; Burgi, H.-B.; Yaghi, O. M. Definitive Molecular Level Characterization of Defects in UiO-66 Crystals. *Angew. Chem., Int. Ed.* **2015**, *54*, 11162–11167.
- (18) Wu, H.; Chua, Y. S.; Krungleviciute, V.; Tyagi, M.; Chen, P.; Yildirim, T.; Zhou, W. Unusual and Highly Tunable Missing-Linker Defects in Zirconium Metal–Organic Framework UiO-66 and Their Important Effects on Gas Adsorption. *J. Am. Chem. Soc.* **2013**, *135*, 10525–10532.
- (19) Hu, Z.; Faucher, S.; Zhuo, Y.; Sun, Y.; Wang, S.; Zhao, D. Combination of Optimization and Metalated-Ligand Exchange: An Effective Approach to Functionalize UiO-66(Zr) MOFs for CO₂ Separation. *Chem. - Eur. J.* **2015**, *21*, 17246–17255.
- (20) Huang, L.; He, M.; Chen, B.; Hu, B. A mercapto functionalized magnetic Zr-MOF by solvent-assisted ligand exchange for Hg²⁺ removal from water. *J. Mater. Chem. A* **2016**, *4*, 5159–5166.
- (21) Liang, W.; Coghlan, C. J.; Ragon, F.; Rubio-Martinez, M.; D’Alessandro, D. M.; Babarao, R. Defect engineering of UiO-66 for CO₂ and H₂O uptake – a combined experimental and simulation study. *Dalton Trans.* **2016**, *45*, 4496–4500.
- (22) Pereira, C. F.; Howarth, A. J.; Vermeulen, N. A.; Paz, F. A. A.; Tome, J. P. C.; Hupp, J. T.; Farha, O. K. Towards hydroxamic acid linked zirconium metal–organic frameworks. *Mater. Chem. Front.* **2017**, *1*, 1194–1199.
- (23) Kim, M.; Cahill, J. F.; Su, Y.; Prather, K. A.; Cohen, S. M. Postsynthetic ligand exchange as a route to functionalization of ‘inert’ metal–organic frameworks. *Chem. Sci.* **2012**, *3*, 126–130.
- (24) Kim, M.; Cahill, J. F.; Fei, H.; Prather, K. A.; Cohen, S. M. Postsynthetic Ligand and Cation Exchange in Robust Metal–Organic Frameworks. *J. Am. Chem. Soc.* **2012**, *134*, 18082–18088.
- (25) Karagiari, O.; Vermeulen, N. A.; Klet, R. C.; Wang, T. C.; Moghadam, P. Z.; Al-Juaid, S. S.; Stoddart, J. F.; Hupp, J. T.; Farha, O. K. Functionalized Defects through Solvent-Assisted Linker Exchange: Synthesis, Characterization, and Partial Postsynthesis Elaboration of a Metal–Organic Framework Containing Free Carboxylic Acid Moieties. *Inorg. Chem.* **2015**, *54*, 1785–1790.
- (26) Li, L.-J.; Liao, P.-Q.; He, C.-T.; Wei, Y.-S.; Zhou, H.-L.; Lin, J.-M.; Li, X.-Y.; Zhang, J.-P. Grafting alkylamine in UiO-66 by charge-assisted coordination bonds for carbon dioxide capture from high-humidity flue gas. *J. Mater. Chem. A* **2015**, *3*, 21849–21855.
- (27) Shearer, G. C.; Vitillo, J. G.; Bordiga, S.; Svelle, S.; Olsbye, U.; Lillerud, K. P. Functionalizing the Defects: Postsynthetic Ligand Exchange in the Metal Organic Framework UiO-66. *Chem. Mater.* **2016**, *28*, 7190–7193.
- (28) Epley, C. C.; Love, M. D.; Morris, A. J. Characterizing Defects in a UiO-AZB Metal–Organic Framework. *Inorg. Chem.* **2017**, *56*, 13777–13784.
- (29) Sun, Y.-J.; Huang, Q.-Q.; Zhang, J.-J. Series of Structural and Functional Models for the ES (Enzyme–Substrate) Complex of the Co(II)-Containing Quercetin 2,3-Dioxygenase. *Inorg. Chem.* **2014**, *53*, 2932–2942.
- (30) Garibay, S. J.; Cohen, S. M. Isoreticular synthesis and modification of frameworks with the UiO-66 topology. *Chem. Commun.* **2010**, *46*, 7700–7702.
- (31) Gross, A. F.; Sherman, E.; Mahoney, S. L.; Vajo, J. J. Reversible Ligand Exchange in a Metal–Organic Framework (MOF): Toward MOF-Based Dynamic Combinatorial Chemical Systems. *J. Phys. Chem. A* **2013**, *117*, 3771–3776.
- (32) Taddei, M.; Tiana, D.; Casati, N.; van Bokhoven, J. A.; Smit, B.; Ranocchiari, M. Mixed-linker UiO-66: structure–property relationships revealed by a combination of high-resolution powder X-ray diffraction and density functional theory calculations. *Phys. Chem. Chem. Phys.* **2017**, *19*, 1551–1559.
- (33) Choi, S.; Kim, T.; Ji, H.; Lee, H. J.; Oh, M. Isotropic and Anisotropic Growth of Metal–Organic Framework (MOF) on MOF: Logical Inference on MOF Structure Based on Growth Behavior and Morphological Feature. *J. Am. Chem. Soc.* **2016**, *138*, 14434–14440.
- (34) During the review process, a similar concept of core–shell type MOF preparation of ligand PSE has been published: Boissonnault, J. A.; Wong-Foy, A. G.; Matzger, A. J. Core–Shell Structures Arise Naturally During Ligand Exchange in Metal–Organic Frameworks. *J. Am. Chem. Soc.* **2017**, *139*, 14841–14844.
- (35) Koh, K.; Wong-Foy, A. G.; Matzger, A. J. MOF@MOF: microporous core–shell architectures. *Chem. Commun.* **2009**, 6162–6164.
- (36) Yoo, Y.; Jeong, H.-K. Heteroepitaxial Growth of Isoreticular Metal–Organic Frameworks and Their Hybrid Films. *Cryst. Growth Des.* **2010**, *10*, 1283–1288.
- (37) Li, T.; Sullivan, J. E.; Rosi, N. L. Design and Preparation of a Core–Shell Metal–Organic Framework for Selective CO₂ Capture. *J. Am. Chem. Soc.* **2013**, *135*, 9984–9987.

(38) Hirai, K.; Furukawa, S.; Kondo, M.; Uehara, H.; Sakata, O.; Kitagawa, S. Sequential Functionalization of Porous Coordination Polymer Crystals. *Angew. Chem., Int. Ed.* **2011**, *50*, 8057–8061.

(39) Szilagy, P. A.; Lutz, M.; Gascon, J.; Juan-Alcaniz, J.; van Esch, J.; Kapteijn, F.; Geerlings, H.; Dam, B.; van de Krol, R. MOF@MOF core–shell vs. Janus particles and the effect of strain: potential for guest sorption, separation and sequestration. *CrystEngComm* **2013**, *15*, 6003–6008.

(40) Hirai, K.; Furukawa, S.; Kondo, M.; Meilikhov, M.; Sakata, Y.; Sakata, O.; Kitagawa, S. Targeted functionalisation of a hierarchically-structured porous coordination polymer crystal enhances its entire function. *Chem. Commun.* **2012**, *48*, 6472–6474.

(41) Deng, H.; Doonan, C. J.; Furukawa, H.; Ferreira, R. B.; Towne, J.; Knobler, C. B.; Wang, B.; Yaghi, O. M. Multiple Functional Groups of Varying Ratios in Metal-Organic Frameworks. *Science* **2010**, *327*, 846–850.